A Wideband Coplanar Waveguide Fed Antenna for Fifth Generation Internet of Things Applications

Rajiv A[a*], **Partibane Bactavatchalame**[r, b]
[a] *R.M.K Engineering College, Kavaraipettai – 601 206, Tamilnadu, India*
[b] *Sri Sivasubramaniya Nadar (SSN) College of Engineering, Kalavakkam – 60311, Tamilnadu, India*

Abstract

A coplanar waveguide (CPW) antenna for 5G internet of things (IoT) communication is designed and experimentally verified in this article. The proposed antenna's radiator comprises of a simple microstrip patch with a single slot, along with cylindrical cut, and a 50 Ω microstrip feed line. This design structure with a slot allows it to resonate in upper frequency ranges and enhance the bandwidth. The construction uses the single layered RT5880 substrate, with two coplanar grounded planes positioned on either side. The measured wide impedance bandwidth of the proposed antenna is less than -10 dB of 133.7% (3 GHz to 15.1 GHz). The parametric evaluation of the proposed antenna design is performed utilizing the length and width of the slots L_s, W_s, and radius R for minimal return loss and consistent performance over entire operating frequency band. The proposed antenna produces omnidirectional radiation patterns across the entire working band, with a peak gain of 6.5 dBi. The suggested antenna has been fabricated and measured, where both the simulated and measured results closely match with one another. The physical dimensions of the proposed antenna are 30 × 24 × 0.5 mm^3. Due to its low cost, wide impedance bandwidth, and seamless integration, this antenna is well-suited for 5G mobile Internet of Things (IoT) applications

Keywords: CPW, IoT, Wideband, 5G applications

1. Introduction

Major breakthroughs in computer networking, microelectronics, and contemporary communication systems are incorporated into Internet of Things (IoT) applications. IoT wireless connectivity standards are swiftly evolving and benefiting as a platform for a wide range of applications that make machines, smart devices, and communications more effective, expand their functionality, and allow them to interact with one another. Internet of Things (IoT) communication refers to the transmission of data between devices via the internet. Depending on the architecture, protocols, and technologies utilized, this communication can take a variety of forms. This technology allows remote Internet-based control of physical sensing and actuating devices. Wireless IoT systems typically work in concordance with wireless routers to enhance signal quality to and from the device they are connected to. Emerging trends in wireless communication technology, notably in the domains of speed, data transmission, and frequency coverage, are shaping the future of improving wireless device performance and usage. Developing wireless communication devices is being researched with an emphasis on smaller size and broader bandwidth for greater transmission speeds. The Internet of Things (IoT) is developing at a rapid pace, which has led to rising demand for compact, cost-effective antennas that can handle 5G and other emerging wireless technologies.

A key factor in this situation is antenna design, which calls for a compact, multiband, broad bandwidth antenna with an underlying framework. This study provides a comprehensive examination of IoT antenna technologies and their importance in ensuring optimal wireless connectivity for various applications. The increasing rise of the Internet of Things requires optimized antenna designs that balance performance, affordability, and integration difficulties. Understanding antenna design trade-offs is critical for IoT applications [1].

Microstrip antennas are popular for their ease of manufacture and compact size, however their narrow bandwidth constrains their applications. UWB is a wireless communication technique that transmits data over an extremely broad bandwidth, usually between 3.1 and 10.6 GHz approved by Federal Communication Commission (FCC). Besides its wide frequency range dispersion, UWB signals are resistant to interference from other wireless technologies. UWB antennas are not feasible for many distinct kinds of communication systems. Furthermore, UWB antennas have a prolonged signal acquisition time and a slow adaption rate. Owing to these problems, UWB systems can only be used for certain communications. In recognition of a number of beneficial characteristics like ease of fabrication, low radiation loss, broadband performance, integration Capability, the utilization of CPW in microstrip patch antennas is highly recommended over alternative feeding methods. Despite this, the CPW-Fed monopole antennas have been determined to be ideal

choices for developing UWB system requirements among numerous variations. One distinct type of electrical planar transmission line that can be built with printed circuit board technology is a coplanar waveguide (CPW). CPW antennas are gaining prominence in the realm of 5G-enabled IoT due to their ease of integration, low cost, and exceptional wideband performance.

The term "being smart," which is defined as a device's capacity to gather on its own and infer information, is the core of the conceptualization of the Internet of Things [2]. These employ antennas to send and receive data which link to a processor that is based on its programming and can carry out a task without demanding any sort of input side. A tricky feat of balance amongst affordability, efficiency, bandwidth, and tangible dimensions confronted frequently by antenna designers, and it is profoundly affected by a variety of factors and is IoT customized.

The development of coplanar waveguide (CPW)-fed slot designs for ultra-wideband (UWB) and wideband antennas has garnered a lot of interest because of their uncomplicated planar construction, ease of manufacture, and broad impedance bandwidth. A variety of slot shapes have been investigated in an effort to reduce antenna size, improve bandwidth, suppress interference, and accomplish multiband performance.

The positive attributes of CPW-fed antennas over traditional ones include wider bandwidth, less dispersion, lower radiation loss, and omnidirectional radiation patterns. To adjust the CPW ground surface, different-shaped slots can be created based on the required bandwidth constraint [3]. CPW-fed antennas feature wide-slot ground, only partially ground, and upwards elongated partial ground approaches in [4-6].Of every conceivable form that originates and is verified for microstrip patch antennas, the square, rectangular, oval, and round-shaped are the most widely utilized [7,8]. For sensing applications, array and slot technology has been deployed to optimize the shape, improve performance, and achieve circular polarization [9,10]. The Internet of Things applications are incredibly diverse, as shown in Figure. 1

In order to achieve various intriguing capabilities for electromagnetic applications, metamaterials, which are a type of artificially structured media with unnatural qualities, are mentioned in [11,12] for wideband applications. Wide-area networks for Internet of Things applications have a lot of exciting possibilities considering how trivial it is to integrate them with electronic systems, as mentioned in [13], and also the wearable antennas. The most recent trends and next technologies can be seen in [14-18].

In order to seamlessly integrate CPW designs into commonplace products, future research can concentrate on transparent and flexible designs utilizing cutting-edge materials like graphene, indium tin oxide, and conductive polymers.This works combines cutting-edge fabrication methods with realistic system concerns for next-generation IoT networks, making a substantial contribution to the fields of wireless communication and antenna engineering [19].A microstrip antenna was successfully produced using a 3D printer, demonstrating its potential as an alternative production method [20].An UWB textile antenna has been proposed for IOT and wearable applications.[21]

In order to satisfy the changing needs of IoT networks, adaptive frequency and radiation pattern control will be made possible by the addition of reconfigurable components, such as MEMS switches or tuneable materials. CPW antennas have the potential to reduce dependency on traditional power sources by using RF energy harvesting to power low-consumption IoT devices. These advancements will establish CPW antennas as a vital component of 5G IoT ecosystems in the future [22], facilitating high-capacity, energy-efficient, and flexible wireless communication systems.

Patch and printed antennas are exceptionally well-suited for extensive IoT networks owing to their beneficial characteristics. According to the literature, these antennas are known for their planar structure, lightweight nature, cost-effectiveness, and ease of integration, making them excellent for Lora WAN and other long-range applications [23]. Their design allows for low-profile and compact form factors, which are required for widespread deployment in smart city infrastructure in both urban and rural areas. Furthermore, their high-performance qualities, such as effective radiation patterns and bandwidth capabilities, ensure dependable long-distance communication [24].

To fully exploit IoT's potential for communication and automation, continuing research and development are advisable where the author presented in depth perspective of antenna's framework [25]. This work presents a compact, dual-band L-shaped slotted antenna for WLAN-based IoT wireless communication. Specifically, the L-shaped stub acts as the main element of radiation, facilitating the generation of these two deep resonances. Parametric analysis was performed to fine-tune the resonant frequencies for WLAN/IoT applications [26]. A small-sized microstrip patch antenna was designed, developed, and evaluated for IoT and ITU applications The T-shaped slotted CPW feed enhances antenna performance by optimizing the radiation aspect, suitable for wireless communication [27-28].

IEEE 802.15.4 requires coverage of significant frequency bands, including 3.4-3.69 GHz, to accommodate future 5G technologies. Wideband and downsized antennas, which cover common frequency bands like Wi-Fi, Bluetooth, Zigbee, LoRa, NB-IoT, and 5G IoT, are an absolute necessity for integrating with IoT devices. In [29],the CPW Fed antenna based on the Locked-Key topology is presented, where the feed line has teeth slits with a bandwidth of 118.2%. A dual-band flexible CPW antenna with an inkjet-printed circular shape attains a bandwidth of 106.7% as well as occupying a larger area [30]. A CPW antenna with four stacked circular patches with a rectangular slot with a footprint of 36mm x 26mm is proposed in [31]. From the literature of [32-41], different designs of CPW-fed antennas have been constructed that have a lower impedance bandwidth compared to the proposed antenna.

While prior CPW-fed slot antenna designs have achieved respectable performance given in Table 1 such as Elliptical and Circular Slots: Due to their intrinsically large

impedance bandwidth and robust omnidirectional radiation, circular slots are among the most prevalent and most used geometries in CPW-fed antennas. As stated in elliptical slots permit many higher-order resonant modes, resulting in even wider bandwidth and lower levels of cross-polarization. Elliptical slots are also more compact than circular ones, which makes them appropriate for handheld and Internet of Things applications [42].

C-Shaped and U-Shaped Slots: By adding extra resonant channels, C-shaped slots are frequently employed to achieve multiband or dual-band-notched characteristics [43]. Conversely, U-shaped and rectangular slots are easy to create and have been widely utilized for band rejection and impedance bandwidth augmentation.

Sinuous and T-Shaped Slots: Meandered or sinuous slot geometries can accommodate a longer current path within a small region, effectively miniaturizing the antenna while retaining wideband operation. Other solutions that use defected ground structures (DGS) or sinuous geometries for miniaturization. typically, do not achieve both ultra-wideband coverage and efficiency in a compact layout. When employing symmetrical arms, such designs may also achieve circular polarization. T-shaped slots are commonly used in the ground plane to improve impedance matching and introduce frequency notches [44-46].

While slot loading is a standard approach for increasing bandwidth in CPW-fed antennas, the proposed design combines a new slot configuration with cylindrical cut enhanced CPW feedline to enable continuous impedance matching from 3.3-15.1 GHz for 5G sub-6 GHz IoT applications.

Despite these advances, most reported designs emphasize merely on bandwidth augmentation or band-notched characteristics, with little regard given to establishing consistent radiation performance across the entire UWB band. Therefore, to accommodate these gaps, the proposed antenna incorporates a rectangular aperture into the CPW feed. This excites several resonant modes, improving the impedance bandwidth and producing uniform radiation behaviour across the operating band. To provide strong electromagnetic coupling and excite various resonant modes, the proposed antenna uses a rectangular slot that is positioned strategically on the radiator and CPW feed.

The coplanar structure and feeding mechanism of CPW antennas provide for greater design flexibility for optimizing bandwidth. Many modules can be constructed on these small devices to increase efficiency, dependability, and robustness for a variety of applications like environmental monitoring, smart cities, smart healthcare, and smart grid. Nonetheless, implementing an effective antenna on all pertinent IoT frequency bands counts as essential, just like with other kinds of IoT requirements. Hence, by eliminating sophisticated construction, we propose a simple wideband CPW-Fed antenna that covers the frequency bands of 5G IoT Sub-6 GHz bands: Band n78 (3.5 GHz), Band n79 (4.7 GHz), Zigbee, Bluetooth, and Wi-Fi.

2. Antenna Design

The suggested antenna's geometry along with the SMA connector is rendered in Figure. 2(a), Figure 2(b). The entire antenna has been constructed on a single-layered RT5880 substrate, whose dielectric constant is 2.2 along with a loss tangent of 0.0009. The height of the substrate is 0.5 mm, and the length and width are 30 mm and 24 mm, respectively. Copper conductive material is used for the center conductor and ground planes.

As the two adjacent ground planes and signal conductor are on the same plane, facilitating integration with other active devices is trivial. A quasi-TEM (Transverse Electromagnetic) mode of propagation, in which the electric and magnetic fields are primarily transverse to the direction of propagation, is supported by the CPW.The addition of a slot to the CPW construction impacts the impedance characteristics of the antenna, impacting the match to the feed line. Ground-gap and line width can be used to control the characteristic impedance. The feeding structure is given by SMA connector to match the impedance of the CPW line and provide efficient power transfer to the antenna.

In Figure. 3, the evolution of the proposed antenna design is proceeded with the basic design (Ant 1) followed by modified CPW antenna design (Ant 2 & Ant 3). The Ant 1 is a conventional CPW-fed 50 Ω patch antenna that comprises a CPW feed of a basic patch with two ground planes on either side as the initial step for the design process. It is observed that L_1 & W_1 play a crucial role in the transient analysis of this antenna, thereby providing S_{11} frequency range from 4 GHz to 7.3 GHz. In Ant 2 the top of the patch is modified by the semi-circle with radius R to observe the improvement in the bandwidth. The S_{11} ranges from 4 GHz to 12 GHz, with a shift in resonance at higher frequencies. The final stage of Ant 3 is made up of adding a slot in the center of the patch. Introduction to slot can change the impedance characteristics of the antenna, affecting the proper match to the feed line. Hence, a wider bandwidth is achieved from 3.6 GHz to 15 GHz, covering various bands, and is suitable for IoT applications. Simulations are performed using ANSYS electronics desktop, while experimental measurements are carried out by fabricating the proposed antenna on RT5880 substrate via a 50 Ω SMA connector. The antenna's performance has been evaluated using a VNA (vector network analyzer) and an anechoic chamber setup to determine its radiation characteristics.

3. Simulations and Experimental Measurements

There are several key trade-offs to consider in terms of antenna parameters. To achieve the desired performance for the specific application, the design as well as optimization requires careful consideration of the length, width, and radius of the CPW antenna. The parametric study in Figure. 4(a), (b), (c) gives an entire view of how these parameters may affect balancing the various performance requirements and constraints for the proposed CPW antenna application.

To further understand the antenna characteristics towards the R in Figure 4(a), it is noted the response of the reflection coefficient is varied from R=2.8 mm to 4.8 mm, where it is observed that wider bandwidth is achieved for R=3.8 mm. In Figure. 4(b), the length of the slot is varied from Ls=4 mm to 6 mm with a transient response of wider bandwidth. Larger slots can also lead to a greater deviation from the desired 50-ohm impedance, making it more challenging to achieve good impedance matching so Ls=5mm is fixed. The width of the slot has also been varied in Figure. 4(c) from Ws=0.5 mm to 1.5 mm. Positioning the slot at different locations along the CPW center conductor or ground planes can shift the antenna's resonant frequency. Wider slots can lead to complex radiation pattern effects where Ws=1mm is selected. In order to construct a wideband CPW antenna that is being simulated, fabricated, and measured, it has the following optimized dimensions are mentioned in Table 2. The proposed antenna is designed and simulated using ANSYS electronic desktop software.

4. Equivalent circuit of the proposed antenna

The proposed antenna reflection value ranges are also validated by mathematical modeling techniques. The main patch is represented by three series RLC resonating circuits in shunt branch. The other two series RLC resonating circuits in the lumped- element equivalent circuit in shunt branch indicating the rectangular and circular cuts in the patch respectively. Moreover, to elucidate the mechanism behind the achievement of bandwidth observed in Ant-3 with the slot introduced in the patch, we have modeled the antenna with a simplified lumped-element circuit which illustrates how an antenna behaves electromagnetically utilizing lumped parts like resistors, inductors, and capacitors.

The RLC equivalent circuit is generated from the manually estimated RLC parameters at these seven frequencies. The circuit is modeled using ADS software and tuned for the reflection coefficient (S_{11}). The tuned RLC equivalent circuit of the proposed antenna is represented in Figure. 5. The ADS software generates the reflection coefficient as displayed in Figure. 6. The reflection coefficient of the proposed antenna has five resonating frequencies with the lowest S_{11} values at 4.07 GHz, 5.78 GHz, 7.625 GHz, 11.315 GHz and 13.655 GHz and has two non-resonating frequencies with the highest S_{11} values at 2.0 GHz, and 18.065 GHz. The impedance plot as illustrated in Figure. 7 shows that imaginary part of the impedance is nearly close to zero at 4.07 GHz, 5.78 GHz, 7.625 GHz, 11.315 GHz and 13.655 GHz, therefore, it behaves as the series resonating circuit at these frequencies in the shunt arms while at the remaining two frequencies 2.0 GHz and 18.065 GHz impedance is complex with sufficient non-zero imaginary parts. Therefore, at these two frequencies, the circuit behaves like a reactive (RC) circuit in the series branch. The values of RLC at all these resonating and non-resonating frequencies are estimated using the simple series resonance circuits and RC reactive circuits are showcased in Table 3.

The HFSS reflection coefficient is compared with the ADS software tuned equivalent circuit reflection coefficients and these are found in excellent agreement in their shape, resonating frequencies, and bandwidths as displayed in Figure 8. This validates the generated equivalent circuit.

For experimental readings the proposed antenna is fabricated, and the antenna's precise readings are taken by connecting the SMA connector carefully to the feed and ground structures. The reflection coefficient is measured using Agilent N5247A VNA. The prototype antenna as well as measurement setup in an anechoic chamber are seen in Figure. 9. The measured S_{11} and gain plot are seen in Figure. 10 & Figure. 11, where the measured bandwidth is from 3 GHz to 15.1 GHz (133.7%), which is better than those when compared with other state of art antennas of [38, 39, 40, 41], and the measured peak gain is 6.5 dBi. However, there is a small deviation in measured results due to dielectric and SMA connector losses.

Simulation and testing were used to assess the proposed antenna's gain in the 3.1–10.6 GHz UWB spectrum. The measurements were conducted in an anechoic chamber setup utilizing the gain comparison method. As the reference antenna, a broadband standard gain horn antenna (10 dBi nominal gain) was positioned 1.5 meters away from the antenna being tested for proposed antenna under test (AUT), meeting the far-field requirements $R > 2D^2/\lambda$. The TRL technique is used to calibrate the VNA with 3.5 SMA calibration kit. As the received power was recorded at specific frequencies, the AUT was positioned on a low-reflection foam platform and rotated azimuthally.

However, in Figure 11 the gain plot shows slight discrepancy low gain dropping below 0 dBi from is due to inefficient Surface Current Distribution of the proposed antenna at 3–4 GHz seem to be less concentrated in radiating regions, which leads to reduced far-field radiation and ineffective modal excitation. The chosen substrate material exhibits a non-negligible loss tangent ($\tan\delta$), which contributes to energy dissipation at lower GHz frequencies. As frequency decreases, the wavelength increases, causing greater interaction with lossy dielectric regions—particularly in the slot-loaded geometry. This diminishes the net radiated power despite good matching. Despite the fact that input power is efficiently received, this weak current distribution further lowers realized gain. The radiation efficiency (η) in this range decreases due to ohmic and dielectric losses. To better understand this efficiency plot and FBR (Front-to-Back Ratio) plots are depicted in Figure 12 & Figure 13 which shows the response efficiency is greater than 85%.

Radiation efficiency accelerates swiftly from ~15% at 2 GHz to over 95% at 4 GHz, with values above 90% throughout the operational span. Higher frequencies (> 14 GHz) show a small reduction, with efficiency dropping to roughly 70% at 16 GHz.

The simulated FBR is quite modest at lower frequencies (< 6 GHz), but considerably increases with frequency, culminating at 37 dB around 10 GHz. This high FBR at mid-band frequencies implies a considerable suppression of backward radiation, which improves antenna transmission.

The FBR steadily drops after the peak, with significant changes at higher frequencies up to 18 GHz.

The antenna achieved a radiation efficiency better than 85% across the whole UWB frequency band

The simulated surface current distribution at the different frequencies, such as 4 GHz, 7.8 GHz, and 14 GHz, is shown in Figure. 14. There appears to be readily apparent high current flow along the feed line, the side edges of the ground, and a radiating patch at lower frequency in Figure 14 (a).

At low frequencies (3-4 GHz), the current is concentrated around the feedline and patch's lower edges, indicating fundamental mode excitation. Radiation is relatively weak, and a considerable percentage of the energy is stored as reactive power, explaining the lower gain even with adequate impedance matching. At mid frequencies (6-8 GHz), strong current concentrations emerge along slot edges and patch boundaries, indicating the excitation of higher order modes. These currents effectively couple with the CPW feed, which boosts radiation efficiency. At high frequencies (>10 GHz), the current becomes more evenly spread across the patch and slot regions, indicating numerous resonant pathways are operating simultaneously. This multi-resonant behavior increases the impedance bandwidth. The observed wideband behavior is mostly due to improved coupling and mode overlapping, which are made possible by the slot region's concentrated currents at mid and high frequencies, which serve as additional radiating sources.
A larger impedance bandwidth is produced by adjusting the parameters where the current density is strongly concentrated. In Figure. 14 (b), Figure. 14 (c), currents are excited by the slot shaped at higher frequencies visible in all areas of radiating structure, which proves for a wider bandwidth.

Figure 15 (a), Figure 15 (b), Figure 15 (c) shows the measured and simulated radiation patterns in the E-plane and H-plane, with three differing resonance frequencies, at 4 GHz, 7.8 GHz, and 14 GHz, which validate the antenna's capacity to provide consistent omnidirectional coverage across the working band. It is seen that measured results agree well with the simulated results. Furthermore, the cross-polarization level in E plane that is primary lobes where the majority of the radiated energy is concentrated in 0 and 180 directions which is satisfactory, while the levels of cross-polarization are at their lowest
Cross-polarization in H-plane is tolerable at 4 and 7.8 GHz, but has significantly high at 14 GHz. This increase is due to the surface current spreads with greater consistency throughout the patch and slot regions at high frequencies (>10 GHz). The HPBW for 4GHz in the E-plane, showing extensive angular coverage across frequencies and steady broadside emission main lobe at (~82°). While in the H-plane, with moderate directivity and front-directed radiation patterns which are narrower with moderate sidelobes (~72°) For 7.8 GHz in E-plane the HPBW narrows (~57°), indicating higher directivity. In H-plane showing Similar narrowing (~55°) with improved beam shaping. At 14GHz In the E-plane there is Further narrowing (~40° HPBW), leading to strong directional radiation. In H-plane around (~38°) with reduced beamwidth for high-gain performance. Consistent omnidirectional coverage is indicated by the comparatively close E-plane and H-plane beamwidths at all frequencies.
Side lobes are well suppressed in all patterns that are measured, remaining below -10 dB, which promotes radiation efficiency and reduces interference.
These findings support the antenna's high gain efficiency and consistent, wide radiation across the UWB band, which makes it ideal for portable wireless systems, IoT devices.
The variations in the pattern that depend on frequency could potentially indicate that the antenna is a part of a wideband system. The proposed antenna is compared to state-of-arts with other wideband antennas in Table 4 to validate in terms of wide bandwidth. CPW antennas are an ideal choice for IoT connectivity owing to their compact size, ease of integration, and high performance. As IoT devices grow more prevalent, the versatility and advantages of CPW antennas make them a vital element in the development of efficient and dependable communication system.

5. Conclusion

In this work, a wideband CPW-fed antenna with modified patch radiator is fabricated on a single-layered RT5880 substrate. The proposed antenna has a wide impedance bandwidth of 133.7% with an operating frequency range from 3 GHz to 15.1 GHz. In addition to wideband, a peak gain of 6.5 dBi is obtained. The overall dimension is 30mm × 24mm × 0.5mm. Both the experimental and modeling study findings convey that the proposed antenna exhibits wide bandwidth and is ideal for IoT applications.

Acknowledgments

There is no acknowledgement for this paper

References

1. Hassan, A., Nizam-uddin, N., Quddus, A., et al. “Designs strategies and performance of IoT antennas: a comprehensive review”, Discover Computing, 28(1), p. 39 (2025). https://doi.org/10.1007/s10791-025-09536-y
2. Ahmed E, Yaqoob I, Gani A, et al. “Internet-of-things-based smart environments: state of the art, taxonomy, and open research challenges”. IEEE Wireless Communications. 2016 Oct;23(5):10-6. https://doi.org/10.1109/MWC.2016.7721736
3. Hakimi S, Rahim SK, Abedian M, et al. “CPW-fed transparent antenna for extended ultrawideband applications”. IEEE Antennas and Wireless Propagation Letters. 2014 Jun 25; 13:1251-4. https://doi.org/10.1109/LAWP.2014.2333091

4. Mahajan RC, Parashar V, Vyas V, et al. “Design and implementation of defected ground surface with modified co-planar waveguide transmission line”. SN Applied Sciences. 2019 Mar;1:1-2. https://doi.org/10.1007/s42452-019-0245-6
5. J. Pourahmadazar, C. Ghobadi, J. Nourinia, et al. “Broadband CPW-fed circularly polarized square slot antenna with inverted-L strips for UWB applications,” IEEE Antennas Wireless Propag. Lett., vol. 10, pp. 369–372, 2011. https://doi.org/10.1109/LAWP.2011.2147271
6. J. Liang, L. Guo, C. C. Chiau, et al, “Study of CPW-fed circular disc monopole antenna for ultra wideband applications,” IEE Proc. Microw., Antennas Propag., vol. 152, no. 6, pp. 520–526, 2005. https://doi.org/10.1049/ip-map:20045179
7. M. Gopikrishna, D. D. Krishna, C. K. Anandan, et al, “Design of a compact semi-elliptic monopole slot antenna for UWB systems,” IEEE Trans. Antennas Propag., vol. 57, no. 6, pp. 1834–1837, Jun. 2009. https://doi.org/10.1109/TAP.2009.2015850
8. Babu GH, Srinivas M, Gnanaprakasam C, et al. “Meander Line Base Asymmetric Co-planar Wave Guide (CPW) Feed Tri-Mode Antenna for Wi-MAX”, North American Public Safety and Satellite Applications. Plasmonics. 2023 Jun;18(3):1007-18. http://dx.doi.org/10.1007/s11468-023-01826-9
9. Kaur A, Malik PK. “Tri state, T shaped circular cut ground antenna for higher ‘X’band frequencies”. In2020 International Conference on Computation, Automation and Knowledge Management (ICCAKM) 2020 Jan 9 (pp. 90-94). IEEE. https://doi.org/10.1109/ICCAKM46823.2020.9051501
10. Schnabel R, Hellinger R, Steinbuch D, et al. “Development of a mid range automotive radar sensor for future driver assistance systems”. International Journal of Microwave and Wireless Technologies. 2013 Feb;5(1):15-23. http://dx.doi.org/10.1017/S1759078712000724
11. Si LM, Zhu W, Sun HJ. “A compact, planar, and CPW-fed metamaterial-inspired dual-band antenna”. IEEE Antennas and Wireless Propagation Letters. 2013 Feb 25;12:305-8. https://doi.org/10.1109/LAWP.2013.2249037
12. Mishra T, Panda SK, Karim MF, et al. “SIW-based slot array antenna and power management circuit for wireless energy harvesting applications”. In Proceedings of the 2012 IEEE International Symposium on Antennas and Propagation 2012 Jul 8 (pp.**1-2**).IEEE. https://doi.org/10.1109/APS.2012.6348552
13. Malik P, Sharma R, Ghosh U, et al. “Internet of Things and long-range antenna's; challenges, solutions and comparison in next generation systems”. Microprocessors and Microsystems. 2023 Nov 1;**103:104934**. https://doi.org/10.1016/j.micpro.2023.104934
14. Kumar S, Tiwari P, Zymbler M. “Internet of Things is a revolutionary approach for future technology enhancement: a review”. Journal of Big data. 2019 Dec;6**(1):1-21**. https://journalofbigdata.springeropen.com/articles/10.1186/s40537-019-0268-2
15. Chauhan DV, Patel A, Vala A, et al. “Microstrip Antenna for Internet of Things (IOT) Applications. Internet of Things Enabled Antennas for Biomedical Devices and Systems”: Impact, Challenges and Applications 2023 May 1 (pp. **129-142**). Singapore: Springer Nature Singapore. http://dx.doi.org/10.1007/978-981-99-0212-5_11
16. Ibrahim AA, Mohamed HA, Abdelghany MA, et al. “Flexible and frequency reconfigurable CPW-fed monopole antenna with frequency selective surface for IoT applications”. scientific reports. 2023 May 24;**13(1):8409**. http://dx.doi.org/10.1038/s41598-023-34917-y
17. Kareem FR, Ibrahim AA, Abdalla MA. “Triple band monopole textile wearable antenna for IoMT application”. IEEE Sensors Journal. 2023 Aug 21. https://doi.org/10.1109/JSEN.2023.3305917
18. Refaat, S.A., Mohamed, H.A., Abdelhady, et al. “A reconfigurable notched band monopole antenna for C-band applications”. International Journal of Electrical and Electronic Engineering & Telecommunications, 2021 10(6), pp.389-396. http://dx.doi.org/10.18178/ijeetc.10.6.389-396
19. Onay MY, Dokmetas B. “3D Printed microstrip antenna for symbiotic communication: WiFi backscatter and bit rate evaluation for IoT”. Internet of Things. 2025 May 19:101643. https://doi.org/10.1016/j.iot.2025.101643
20. B. Dokmetas, G. O. Arican and B. A. Yilmaz, "A Folded Pyramid-Shaped Microstrip Antenna with Improved Bandwidth," 2024 IEEE International Symposium on Antennas and Propagation and INC/USNC-URSI Radio Science Meeting (AP-S/INC-USNC-URSI), Firenze, Italy, 2024, pp. 1273-1274. https://doi.org/10.1109/AP-S/INC-USNC-URSI52054.2024.10686622
21. Sharma MD, Yadav A, Singhal S, et al., “CPW Fed Textile UWB Antenna for IoT and Wearable Applications”. Scientia Iranica. 2025 Jan 13. https://doi.org/10.24200/sci.2025.64547.9070
22. Pawar AN, Deosarkar SB. “A comprehensive review of different antennas for IoT applications”. Wireless Networks. 2025 Feb;31(2):1449-61. https://doi.org/10.1007/s11276-024-03844-9
23. Yahya MS, Soeung S, Rahim SK, et al., “LoRa microstrip patch antenna: a comprehensive review”. Alexandria Engineering Journal. 2024 Sep 1; 103:197-221. https://doi.org/10.1016/j.aej.2024.06.017
24. Anchidin L, Lavric A, Mutescu PM, et al., “The design and development of a microstrip antenna for internet of things applications”. Sensors. 2023

Jan 17;23(3):1062. https://doi.org/10.3390/s23031062
25. Khan S, Mazhar T, Shahzad T, et al., "Antenna systems for IoT applications: a review". Discover Sustainability. 2024 Nov 15;5(1):412. https://doi.org/10.1007/s43621-024-00638-z
26. Panda JR, Behera BK, Dash SK, et al., "CPW-fed Printed Square Slotted Antenna for IoT/WLAN Applications". In 2024 Fourth International Conference on Advances in Electrical, Computing, Communication and Sustainable Technologies (ICAECT) 2024 Jan 11 (pp. 1-4). IEEE. https://doi.org/10.1109/ICAECT60202.2024.10468798
27. Srinivas M, Reddy GR, Sangeethapriya S, et al., "Design and fabrication development of slotted T-shaped patch antenna with symmetrical CPW feed for IOT and ITU applications". Plasmonics. 2024 Nov 4:1-0. https://doi.org/10.1007/s11468-024-02553-5
28. Y. Xue, R. Yan, W. Huang, et al., "A wideband CPW slot antenna by using conductor-backed coplanar feeding," Sensors, vol. 24, no. XX, 2024. https://doi.org/10.1016/j.heliyon.2024.e40628
29. Jameel, M.S., Mezaal, Y.S. and Atilla, D.C. "Miniaturized coplanar waveguide-fed UWB antenna for wireless applications". Symmetry 2023, 15(3), p.633. https://doi.org/10.3390/sym15030633
30. Kirtania, S.G., Younes, B.A., Hossain, A.R., et al., "CPW-fed flexible ultra-wideband antenna for IoT applications". Micromachines 2021, 12(4), p.453. https://doi.org/10.3390/mi12040453
31. Gupta N, Saxena J, Bhatia KS, et al., "A compact CPW-fed planar stacked circle patch antenna for wideband applications". Wireless Personal Communications. 2021 Feb;116(4):3247-60. https://doi.org/10.1007/s11277-020-07847-5
32. Kundu, S. And Jana, S.K., "A leaf-shaped CPW-fed UWB antenna for GPR applications". Microwave and Optical Technology Letters 2018, 60(4), pp.941-945. https://doi.org/10.1002/mop.31089
33. Ahmad, S., Vargas, D.S., Ghaffar, A., et al., "A Compact Size CPW-Fed Ultra-Wideband (UWB) Antenna for Wireless Networks". In 2022 March 16th European Conference on Antennas and Propagation (EuCAP) (pp. 1-5). IEEE. https://doi.org/10.23919/EuCAP53622.2022.9769083
34. Sreenath, S., Ashkarali, P., Thomas, P., et al., "CPW-FED compact bent monopole antenna for UWB applications". Microwave and Optical Technology Letters 2013, 55(1), pp.56-58. https://doi.org/10.1002/mop.27252
35. Koziel, S. and Bekasiewicz, A., "A structure and simulation-driven design of compact CPW-fed UWB antenna". IEEE Antennas and Wireless Propagation Letters 2015, 15, pp.750-753. https://doi.org/10.1109/LAWP.2015.2471848
36. Sawant, K.K. and Kumar, C.S., "CPW fed hexagonal micro strip fractal antenna for UWB wireless communications". AEU-International Journal of Electronics and Communications 2015, 69(1), pp.31-38. https://doi.org/10.1016/j.aeue.2014.07.022
37. Fallahi, H. and Atlasbaf, Z., "Bandwidth enhancement of a CPW-fed monopole antenna with small fractal elements". AEU-International Journal of Electronics and communications 2015, 69(2), pp.590-595. https://doi.org/10.1016/j.aeue.2014.11.011
38. Omar AA, Abu Safia O, Nedil M. "UWB coplanar waveguide-fed coplanar strips rectangular spiral antenna". International Journal of RF and Microwave Computer-Aided Engineering. 2017 Sep;27(7):e21115. https://doi.org/10.1002/mmce.21115
39. Pandey D, Sharma V, Kundu S. "CPW fed Heart shaped Antenna for Ultra-Wide Band Applications". In 2023 3rd International Conference on Range Technology (ICORT) 2023 Feb 23 (pp. 1-4). IEEE. https://doi.org/10.1109/ICORT56052.2023.10249142
40. Kundu S, Kundu S. "A compact U-shaped antenna with bandwidth enhancement for ultra-wideband communication". In 2021 2nd international conference on range technology (ICORT) 2021 Aug 5 (pp. 1-4). IEEE. https://doi.org/10.1109/ICORT52730.2021.9581344
41. Tan MT, Li JQ, Jiang ZY. "A miniaturized ultra wideband planar monopole antenna with L shaped ground plane stubs". International Journal of RF and Microwave Computer Aided Engineering. 2019 Nov;29(11):e21935. https://doi.org/10.1002/mmce.21935B.
42. Maity and S. K. Nayak, "A super wideband CPW-fed elliptical slot monopole antenna for wireless applications," Progress in Electromagnetics Research C, vol. 130, pp. 139–154, Feb. 2023. https://www.jpier.org/PIERC/pier.php?paper=22120505
43. Z. Deng, C. Lai, Y. Wang, et al., "Design of a quadruple band-notched ultra-wideband (UWB) antenna using curled C-shaped structures and interdigital inductance slots", Electronics, vol. 11, no. 23, art. 3949, Nov. 2022. https://doi.org/10.3390/electronics11233949
44. A. U. Bhobe, C. L. Holloway, M. Piket-May, et al., "Wide-Band Slot Antennas With CPW Feed Lines — Hybrid and Log-Periodic Designs", IEEE Trans. Antennas Propag., vol. 52, no. 10, pp. 2545–2554, Oct. 2004. (Classic, widely cited; discusses slot shapes and DGS techniques.) https://ieeexplore.ieee.org/document/1341608

45. J. Gamec, M. Repko, M. Gamcová, I. et al., "Low profile sinuous slot antenna for UWB sensor networks," Electronics, vol. 8, no. 2, art. 127, 2019. https://doi.org/10.3390/electronics8020127
46. Z. Ding, H. Wang, S. Tao, et al., "A novel broadband monopole antenna with T-slot, CB-CPW, parasitic stripe and heart-shaped slice for 5G applications," Sensors, vol. 20, no. 24, art. 7002, Dec. 2020. https://doi.org/10.3390/s20247002

Biographies:

Rajiv A received the B.E. (ECE) and M.E. (Embedded System Technologies) degrees from Anna University, Chennai, India in 2007 and 2010 respectively. Currently he is pursuing Ph.D in Anna University and working as Assistant Professor in Department of Electronics and Communication Engineering, R.M.K Engineering College, Kavaraipettai. His research interests include RF and Microwave Engineering, Antenna Design, Embedded Systems.

Bactavatchalame Partibane received his BE degree in ECE from Madras University, Chennai, in 1999, and the MTech degree in ECE from Pondicherry University, Pondicherry, in 2003. Further, he obtained doctoral degree from Anna University, Chennai in 2017. He currently holds an academic post as Associate Professor in the department of ECE, SSN Institutions. His research interests include Wireless Communication and Networks, Antenna Engineering and Security in Ad hoc and Sensor Network.

able 1. Types of slot Geometry

Ref.	Type of Slot Geometry	Bandwidth (GHz)	Primary Specifications
[42]	Circular/ Elliptical	1.613–26.357	Stable omnidirectional radiation, Super-wideband; compact; low cross-polarization.
[43]	C-shaped	2.95–12	Band-notch capability; multiband rejection via C-slots.
[44]	Rectangular with DGS	3–14	UWB with improved matching using defected ground structures.
[45]	Sinuous (Meandered)	0.1–6	Intrinsic UWB; miniaturization via long current paths.
[46]	T-shaped (Ground Plane / Feed)	4.69–8.71	T-slot improves matching/creates notch or broadband response.

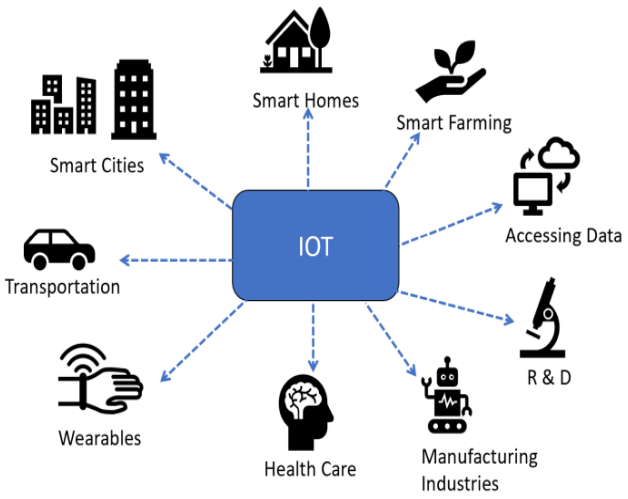

Figure 1. IoT applications

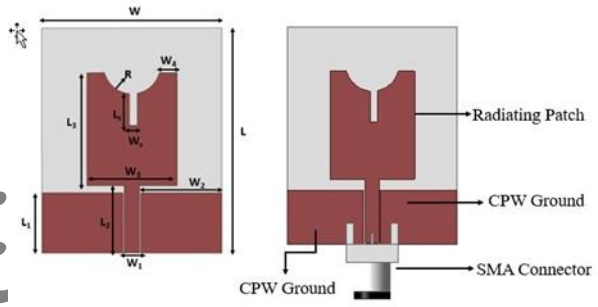

Figure 2. (a) Configuration of proposed (b) Schematic view with SMA connector

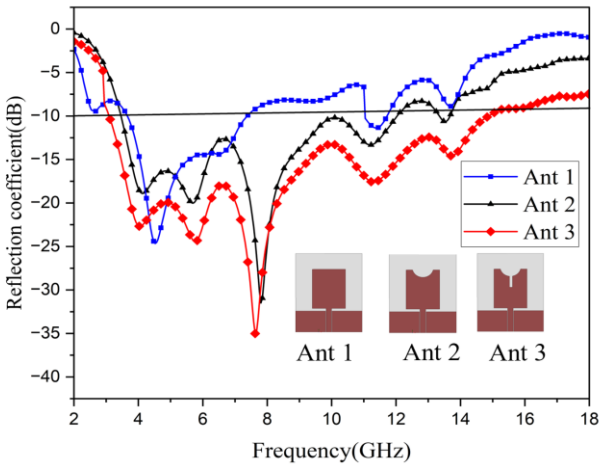

Figure 3. Evolution of the proposed antenna with different antenna stages(a) Only patch
(b) Patch with Cylindrical cut
(c) Patch with cylindrical cut & slot

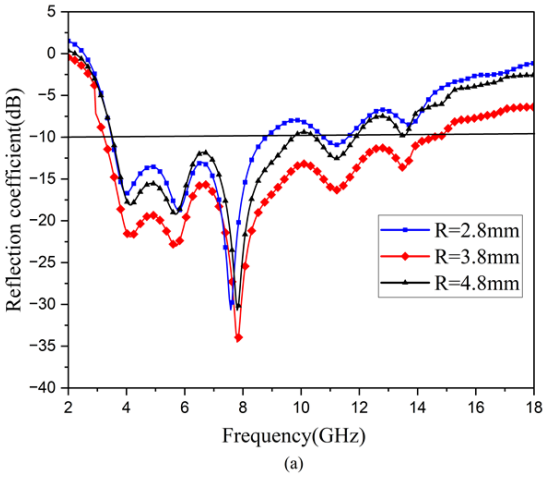

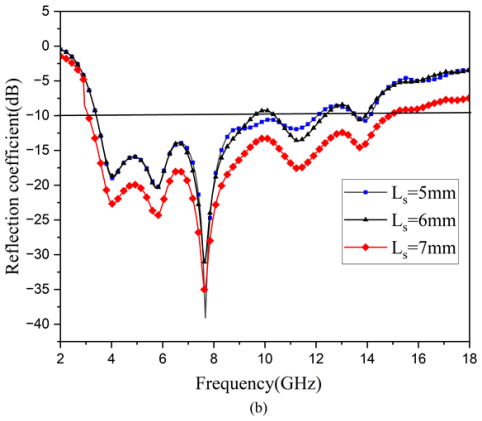

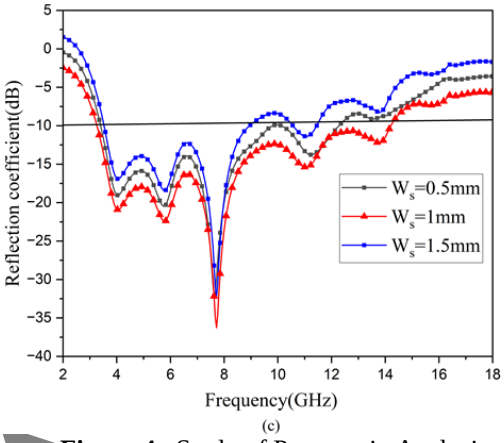

Figure 4. Study of Parametric Analysis on (a) Radius R (b) Length of the slot L_s (c) Width of the slot of W_s

Table 2. Dimensions of the Proposed Antenna (units in mm)

Parameters	Values	Parameters	Values
L	30	W_1	2
W	24	W_2	10.8
L_1	7.5	W_3	12
L_2	10	W_4	2.2
L_3	15	W_s	1
L_s	5	R	3.8

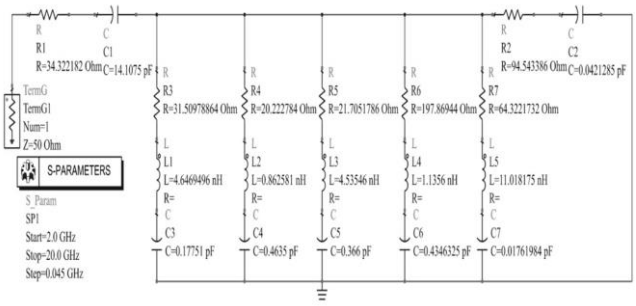

Figure 5. Portrays a part-by-part analogy between an antenna and a lumped-element equivalent circuit.

Table 3. RLC parameters of the equivalent circuit

Resonance frequency (GHz)	RLC values
2.0 (non-resonating)	R_1 = 34.322 Ω; C_1 = 14.1075 pF
4.07	R_2 = 31.509 Ω; L_2 = 4.647 nH; C_2 = 0.1775 pF
5.78	R_3 = 20.222 Ω; L_3 = 0.8625 nH; C_3 = 0.4635 pF
7.625	R_4 = 21.705 Ω; L_4 = 4.5354 nH; C_4 = 0.366 pF
11.315	R_5 = 197.8694Ω; L_5 = 1.1356 nH; C_5 = 0.4346 pF
13.655	R_6 = 64.322 Ω; L_6 = 11.018 nH; C_6 = 0.0176 pF
18.075(non-resonating)	R_7 = 94.543 Ω; C_7 = 0.0421 pF

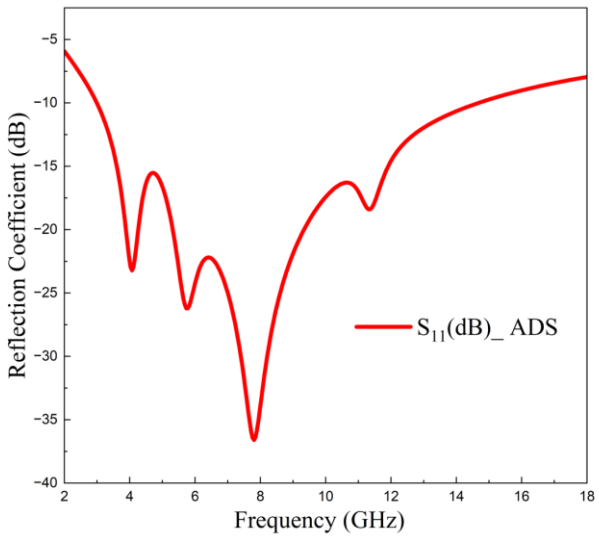

Figure 6. ADS-software simulated reflection coefficient of the proposed antenna

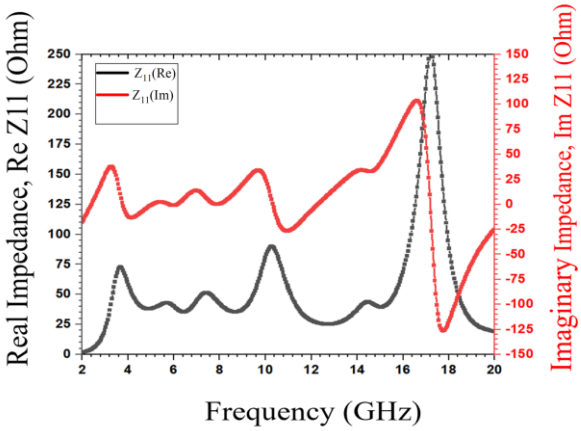

Figure 7. Impedance plot of proposed antenna.

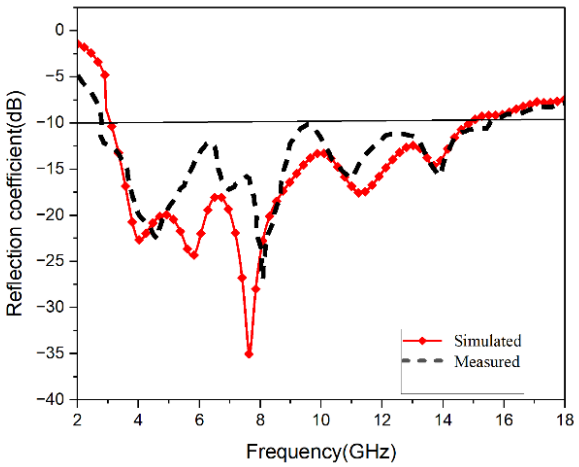

Figure 10. Simulated and Measured Reflection Coefficient

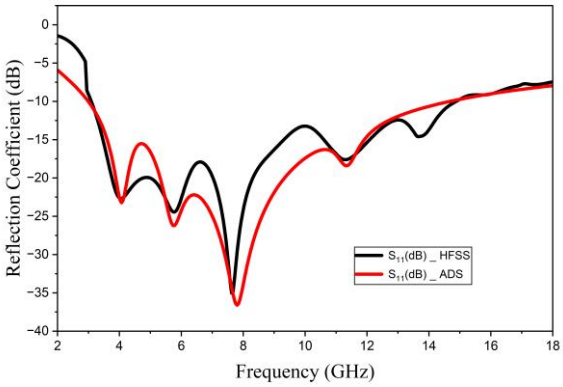

Figure 8. RLC equivalent Circuit validation of proposed antenna

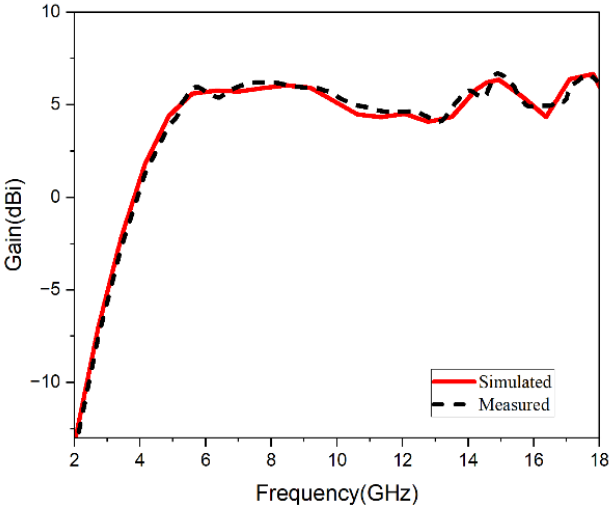

Figure 11. Simulated and Measured Gain

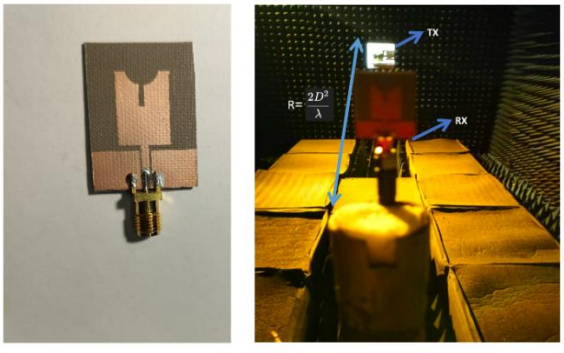

Figure 9. (a) Prototype of fabricated antenna (b) anechoic chamber setup

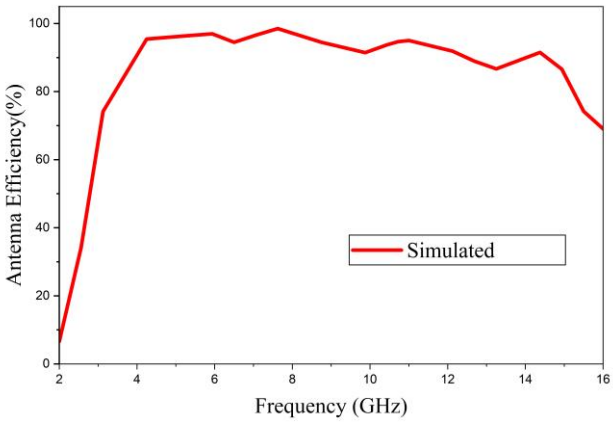

Figure 12. Simulated Efficiency

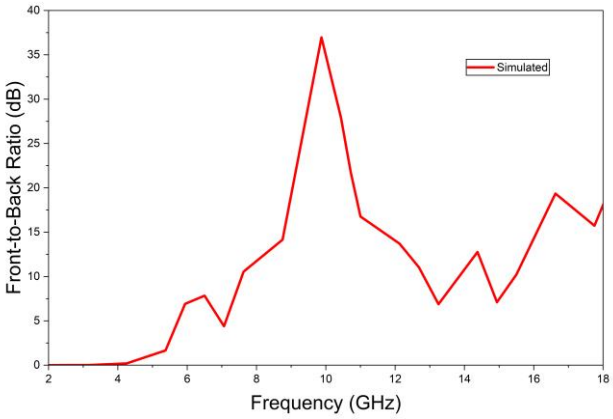

Figure 13. Front-to-Back Ratio

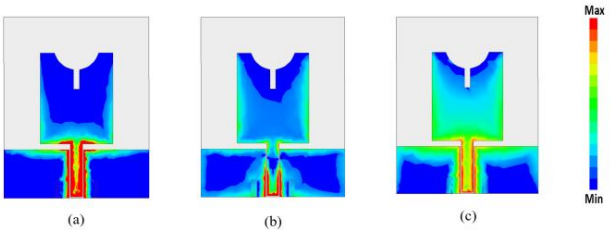

Figure 14. Surface Current distributions at (a) 4 GHz (b) 7.8 GHz (c) 14 GHz

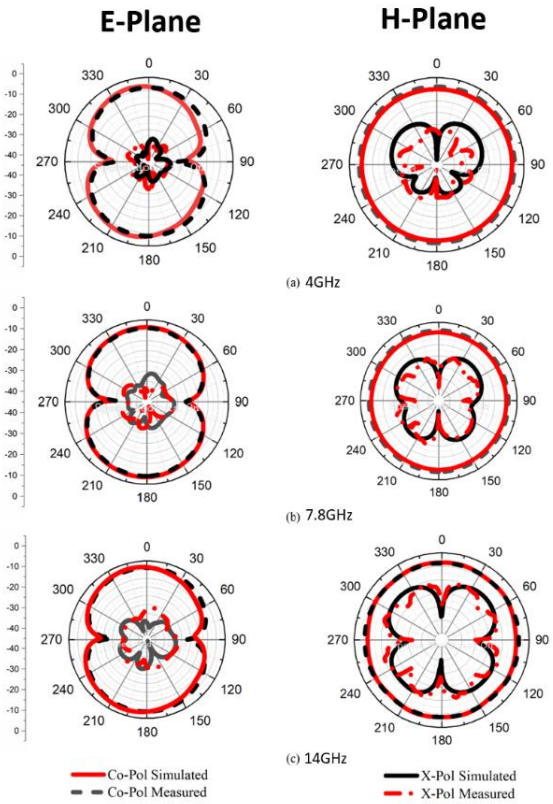

Figure 15. Radiation Patterns

Table 4. Performance Comparison of the Proposed Antenna with reference antennas

Ref	Frequency Range (GHz)	Bandwidth (%)	Substrate Used	Antenna Size(mm^3) L × W × H	Gain (dB)
[29]	3.58-14	118.54	FR4	27 × 25 ×1.5	4.7
[30]	3.04–10.70	106.7	Flexible polyethylene terephthalate (PET) substrate	47 × 25 × 0.135	3.94
[31]	2.59-7.61	98.3	FR4	36 × 26	9.3
[32]	3.1-10.6	109.4	FR4	38.31 × 34.52 × 0.8	2-5
[33]	3-11	114.2	FR4	31.68 × 23.76 ×1.6	4.1
[34]	3.1-10.8	110.7	FR4	35 × 35 × 1.6	2.5
[35]	3-11.2	115.4	Taconic RF-35	20.7 × 20.2 × 0.762	-
[36]	3.1-10.6	109.4	Polyamide	26 × 30 × 1.53	-
[37]	3.1-10.6	109.4	FR4	25 × 25 × 1	3.5
[38]	3.5 -10	96.2	RO4003C	50 × 40	4.7
[39]	2.62-11.62	126.5	FR4	40 × 36 × 0.8	4.15
[40]	3-12.4	122	FR4	36 × 22 × 0.8	1.4-4.8
[41]	2.7-11.85	125	FR4	25 × 25 × 1	3.2
Proposed	**3-15.1**	**133.7**	**RT 5880**	**30 × 24 × 0.5**	**6.5**

*Corresponding author: rajiv.angel25@gmail.com